The impact of protection system failures and weather exposure on power system reliability

Erlend Sandø Kiel
Department of Electric Power Engineering
NTNU - Norwegian University of Science and Technology
Trondheim, Norway
erlend.kiel@ntnu.no

Gerd Hovin Kjølle
Department of Electric Power Engineering
NTNU - Norwegian University of Science and Technology
Trondheim, Norway

***Abstract*—Extreme weather is known to cause failure bunching in the electrical transmission system. However, protection systems can also contribute to the worsening of the system state through spontaneous, missing or unwanted operation of the protection system. The latter two types of failures only occur when an initial failure has happened, and thus is more likely to happen when the probability of failure of transmission lines is high, such as in an extreme weather scenario. This causes an exacerbation of failure bunching effects, increasing the risk of blackouts, or High Impact Low Probability (HILP) events. This paper describes a method to model transmission line failure rates, considering both protection system reliability and extreme weather exposure. A sample case study is presented using the 6 bus RBTS test-system. The case study, using both an approximate method as well as a time-series approach to calculate reliability indices, demonstrates both a compact generalization of including protection system failures in reliability analysis, as well as the interaction between weather exposure and protection system failures and its impact on power system reliability indices. The results show that the inclusion of protection system failures can have a large impact on the estimated occurrence of higher order contingencies for adjacent lines, especially in periods of high weather exposure.**

Keywords—protection systems, failure bunching, extreme weather, exposure, reliability, HILP, extraordinary events.

I. INTRODUCTION

Society is dependent on a reliable supply of electricity for its normal operation, and thus power outages can have severe consequences. Environmental factors have shown to be one of the main causes to major blackouts [1]–[5]. The increased probability of one or more component failures in a short period of time due to extreme weather has been termed failure bunching, and models have been developed to capture such effects in power system reliability studies both using analytical techniques and Monte Carlo approaches [6]–[8]. Large blackouts are often a consequence of complex series of events, such as cascading failures [9]. A distinction in the structure of cascading blackouts is made in [10] between a triggering event, which can be simple component failure(s), and generations of propagating events, caused by preceding events and a change in the power system state. One of the causes of propagating events is the malfunction of protection systems [4], [9], [11]. In previous works it has been shown that protection system reliability can have a notable impact on reliability of supply [12].

The combination of failure bunching effects and protection system failures may cause the system to end up in a less desired state than what was initially expected. The contribution of this paper is to formulate general and compact equations to incorporate protection system failures in reliability analysis, based on [12]. The novelties in this paper are 1) Based on graph theory, finding paths of possible propagation of failures between transmission lines. 2) These equations are then developed to be applicable to time-series of failure probability of transmission lines, which can be used to capture the interaction between protection system failures and failure bunching effects due to weather. The aim of the paper is not to fully capture the complex chains of events which can be found in a power system cascade, but rather to incorporate the early steps of such events combining the two phenomena.

The paper is structured as follows: In Section II, previous work on failure bunching effects and protection system reliability is presented, as well as a short review of graph theory and its use in this study of power systems reliability. In Section III, a general and compact method for calculating reliability indices including protection system failure and maloperation is presented. Section IV presents a case study where the method is applied, before the paper is concluded in section V.

II. FAILURE BUNCHING AND PROTECTION FAILURES

Harsh weather has long been known to cause common cause failures within short periods of time, often termed failure bunching. One way of incorporating such effects is to use multi-state Markov models or similar approximate methods when calculating reliability, another is to utilize Monte Carlo simulation techniques [3], [13], [14]. In [13], the effect of failure bunching due to wind exposure is captured using historical failure data and a Bayesian updating scheme to estimate annual wind dependent failure rates of transmission lines. The annual failure rate is then spread out in time by combining fragility curve modeling and a dataset of historical wind speeds for the lines in question. This results in hourly time-series of wind dependent failure probability for the lines. The time-series of historical failure probability in [13] is further used together with a Monte Carlo-based tool to calculate system consequences in terms of interrupted power and interruption costs in [15].

In [8] an analytical technique is used to calculate time-series of expected unavailability of transmission lines due to wind rather than using a Monte Carlo approach. For each hour, the probability of failure is paired with a distribution of outage duration for the relevant type of failure. An iterative algorithm then appends the probability of the component being unavailable due to a failure at a specific time for a given number of hours ahead in time. A contingency enumeration approach, defining outage combinations as cutset structures [16], [17] is then used together with the time-series of expected unavailability of transmission lines to calculate the reliability index annual energy not supplied (ENS) for the system.

Protection systems are expected to be both dependable and secure [12]. Missing operation of the protection system

The research leading to these results has received funding through the project "Analysis of extraordinary events in power systems" (HILP) (Grant No. 255226), co-funded by the Research Council of Norway, Statnett and Fingrid.

occurs if it fails to react appropriately to a situation it is designed to respond to and would be a shortfall of the dependability of the system. Similarly would an unwanted operation occur if the protection system reacts to conditions it is not designed to react to, and is a shortfall of the security of the system [12]. These two elements of reliability were the basis in [12] to construct different scenarios in which protection system reliability can cause a transmission line to be isolated from the network. This gave rise to four fault types [12]: Fault type 1 (FT1) is the failure rate of the transmission line in focus. Fault type 2 (FT2) represents failures due to the spontaneous unwanted operation of a line's own protection system. Fault type 3 (FT 3) is explained by a situation where a failure occurs on a neighboring line but is not correctly cleared due to missing operation of the neighboring line's protection system, and thus causes the line in focus to be isolated from the system. Fault Type 4 (FT4) is a result of a fault on the neighboring line that is correctly cleared by the neighboring line's protection system but causes an unwanted non-selective tripping of the line in focus. An equivalent failure rate for each line is then constructed as a summation of these four failure type contributions. The method is a contingency enumeration approach, where an approximate system reliability evaluation [18] is used to obtain reliability indices for predefined minimal cutsets. A more detailed presentation of the approach can be found in [12].

The role of protection systems makes it necessary to systematically consider the adjacency between transmission lines. Much of the literature on cascades employs complex network theory and graph-theoretic approaches to identify important generators, transformers, substations and lines, to mention a few, in the power system [19]–[21]. The power system lends itself to a graph-based representation, where vertices (V) are considered as buses and edges (E) are considered as undirected edges between the buses. A graph (G) is an object consisting of an ordered vertex set and an edge set joining the vertices, as seen in (1)–(3), where n is the number of vertices in the graph and m is the number of edges in the graph, see e.g. [22], [23].

$$G = (V, E) \tag{1}$$

$$V = \{c_1, c_2 \dots c_n\} \tag{2}$$

$$E = \{\{u_1, v_1\}, \{u_2, v_2\} \dots \{u_m, v_m\}\} \tag{3}$$

In the following, the graph-based representation of relationships is a useful tool to incorporate protection system failures into power system reliability analysis.

III. Method

The aim of the method described in this paper is to create compact and general equations to calculate the impact of protection system failures on power systems reliability evaluation, based on [12]. The method is formulated using both an approximate systems reliability approach [17], [18] in Sec. III.A, and a time-series approach [8] in Sec. III.B. The idea behind the method in this paper is to see vertices as transmission lines and edges as dependencies between transmission lines, rather than buses and transmission lines, respectively. This structure can then be utilized to calculate the contribution to failure rates at a given transmission line, given failures at adjacent lines.

When including protection system failures into the system, we consider two different types of lines in each case: the target line i, for which we wish to calculate the failure rates, and the source line j, which is adjacent to the target line and contributes to the failure rate of the target line through propagation of protection system faults. The target- and source lines are adjacent lines if they are connected to a common bus, as seen in Fig. 1. The subscript l is used when it is not specific if the line is a target or a source line.

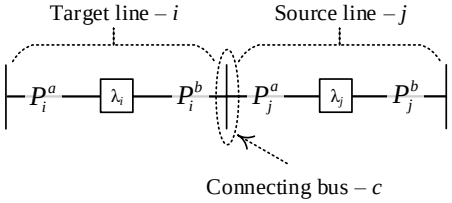

Fig. 1. Two adjacent transmission lines, *i*, *j*.

A line is associated with a protection system on each end of the line. These are referred to as the a- and b-side protection systems, represented as the set $s = \{a, b\}$ for simplicity. For a line we consider the failure rate of the line λ_l, and the two protection systems, P_l^s. The protection systems have three parameters, 1) a specific annual failure rate, λ_l^s, 2) a conditional probability of missing operation, $P_l^{s,m}$, if the line experience a failure, and 3) upon a correctly cleared failure at an adjacent line, a conditional probability of unwanted non-selective tripping at the target line, $P_l^{s,u}$. The restoration time, r, is denoted with a subscript indicating which line is considered, and a superscript indicating which fault type it is applicable to. All line- and protection system specific information is represented as ordered column vectors.

We are primarily concerned with how maloperation of the protection system of one transmission line can cause an adjacent line to be isolated from the system. The system can initially be considered a graph G, where each edge $e = \{u, v\}$ represents a transmission line, and the buses are represented by vertices, which are unique observations of u and v. We let u represent the a-side connecting bus of a line, and v to represent the b-side connecting bus. An adjacency matrix indicates connections between vertices, and we wish to represent our system in a form where vertices are transmission lines and edges are directed paths of fault propagation between the lines. An adjacency matrix is constructed for each side of the source line, $\boldsymbol{A}^s$ in (4), to take into account which side of the source line is connected to the target line. The adjacency matrix is an ordered $l * l$-matrix, where rows represent a target line i and columns represent a source line j. If line j is connected to line i through its *s*-side, it is marked with a digit 1 in the appropriate element, 0 otherwise. Matrices and vectors are typeset in bold, while specific elements of a matrix or vector, or scalar values are denoted with regular fonts.

$$\boldsymbol{A}^s = \left[a_{i,j}^s\right] = \begin{bmatrix} a_{1,1}^s & \cdots & a_{1,j}^s \\ \vdots & \ddots & \vdots \\ a_{i,1}^s & \cdots & a_{i,j}^s \end{bmatrix} \tag{4}$$

$$where\ s = \{a, b\}$$

$$a_{i,j}^a = \begin{cases} 1 & u_j \in \{u_i, v_i\} \\ 0 & \text{Otherwise} \end{cases}$$

$$a_{i,j}^b = \begin{cases} 1 & v_j \in \{u_i, v_i\} \\ 0 & \text{Otherwise} \end{cases}$$

The adjacency matrix can then be further modified to incorporate the probability that a failure on a source line will propagate to a target line. From the initial equations in [12],

we know that only FT3 and FT4 stem from adjacent lines and as such these fault types will receive the primary focus.

FT3 is related to a failure on an adjacent line, which is not correctly cleared by the adjacent line's protection system. The probability of missing operation of the protection system on the s side for a given line is represented by the column vector $\boldsymbol{P_l^{s,m}}$. Adjacency matrices can then be modified to incorporate the probability of a failure propagating through the FT3 mechanism in (5).

$$\boldsymbol{PT3} = [pt3_{i,j}] = \sum_{s\in\{a,b\}} \left[\begin{bmatrix} a_{1,1}^s & \cdots & a_{1,j}^s \\ \vdots & \ddots & \vdots \\ a_{i,1}^s & \cdots & a_{i,j}^s \end{bmatrix} \cdot \begin{bmatrix} p_1^{s,m} \\ \vdots \\ p_l^{s,m} \end{bmatrix} \right] = \sum_{s\in\{a,b\}} \left[\boldsymbol{A^s} \cdot \boldsymbol{P_l^{s,m}} \right] \quad (5)$$

PT3 only takes into consideration the properties of line j's protection systems. The same probability matrix for FT4, a failure on the source line causing an unwanted non-selective tripping of the protection systems at the target line, PT4, must consider protection system properties of both the target and the source line. The probability of line j successfully clearing a failure on its own line is calculated in the inner bracket in (6). The matrix is then transposed to calculate the probability of an unwanted non-selective tripping of line i before the matrix is transposed back into its original direction. Note that the probability of unwanted spontaneous operation is represented by a single column vector since the target line response is side-independent, where $\boldsymbol{p_l^u} = P\left(p_l^{a,u} \cup p_l^{b,u}\right)$.

$$\boldsymbol{PT4} = [pt4_{i,j}] = \sum_{s\in\{a,b\}} \left[\left[\boldsymbol{A^s} \cdot \left(1 - \boldsymbol{P_l^{s,m}}\right) \right]^T \cdot \boldsymbol{P_l^u} \right]^T \quad (6)$$

Matrices representing the probability of different fault types propagating from a source line to a target line have now been established. This can be applied to calculate systems reliability indices for cutsets. Two methods are presented here. First, an approximate method of systems reliability using annual failure rates including protection system failures. Secondly, a method to calculate time series of probability of failure due to different fault types, which can be used together with [8] to calculate unavailability of cutsets.

A. Approximate method

This approach starts by calculating the equivalent failure rate of each line, and do this by considering each line a target line. The equivalent failure rate is calculated based on the failure rate of the line itself (FT1) and its protection systems (FT2), and the fault types FT3 and FT4 propagating from adjacent lines. FT1 and FT2 are only dependent on information of the line itself and is repeated for reference here (7)-(8). FT3 and FT4 is calculated by using the associated probability matrices (9)-(10). For FT3 and FT4 we summarize values along the j -axis of the matrix resulting from multiplication of the probability matrix with the adjacent line failure rates. This gives us a vector of all FT3 and FT4 failure rate contributions from all source lines at the target line.

$$\boldsymbol{FT1_i} = \boldsymbol{\lambda_l} \quad (7)$$

$$\boldsymbol{FT2_i} = \sum_s \boldsymbol{\lambda_l^s} \quad (8)$$

$$\boldsymbol{FT3_i} = \sum_j [\boldsymbol{PT3} \cdot \boldsymbol{\lambda_l}] \quad (9)$$

$$\boldsymbol{FT4_i} = \sum_j [\boldsymbol{PT4} \cdot \boldsymbol{\lambda_l}] \quad (10)$$

Equivalent failure rates, incorporating protection system failures is then calculated as $\boldsymbol{\lambda_l'}$ in (11).

$$\boldsymbol{\lambda_l'} = \boldsymbol{FT1_i} + \boldsymbol{FT2_i} + \sum_j \left[[\boldsymbol{PT3} + \boldsymbol{PT4}] \cdot \boldsymbol{\lambda_l} \right] \quad (11)$$

From this, we can obtain equivalent unavailability and repair rates for all target lines in (12)-(13), where elementwise Hadamard operations are performed when calculating unavailability for FT1, FT2 and equivalent repair rates. Note that the unavailability due to FT4 is dependent on the switching time of the line's own protection system, hence the double transpose.

$$\boldsymbol{U_l'} = \boldsymbol{FT1_l} \circ \boldsymbol{r_l^{FT1}} + \boldsymbol{FT2_l} \circ \boldsymbol{r_l^{FT2}} + \sum_j \left[\left[\boldsymbol{PT3} \cdot \boldsymbol{r_l^{FT3}} + \left[\boldsymbol{PT4}^T \cdot \boldsymbol{r_l^{FT4}} \right]^T \right] \cdot \boldsymbol{\lambda_l} \right] \quad (12)$$

$$\boldsymbol{r_l'} = \boldsymbol{U_l'} \oslash \boldsymbol{\lambda_l'} \quad (13)$$

We have now established vectors containing reliability indices for single lines. We can then calculate second order cutsets involving two lines x and y in a general form, avoiding a distinction in equations between adjacent and non-adjacent lines by utilizing the matrix of adjacency adjusted probabilities. If two lines in a cutset are adjacent and they experience a FT3 or a FT4 where the source line is the other line in the cutset, they will both surely be unavailable. This means that these dependent failures should be deducted from the multiplicative part of the equations for failure rates and repair times, creating adjustments for failure rates and unavailability for individual lines in the cutset (14)-(15) before calculating the expected restoration time of the cutset after adjustments in (16).

$$\lambda_{x,y}^a = \left(pt3_{x,y} + pt4_{x,y}\right) \cdot FT1_y \quad (14)$$

$$U_{x,y}^a = \left(pt3_{x,y} \cdot r_y^{FT3} + pt4_{x,y} \cdot r_x^{FT4}\right) \cdot FT1_y \quad (15)$$

$$r_{x,y}^n = \frac{U_x' - U_{x,y}^a}{\lambda_x' - \lambda_{x,y}^a} \quad (16)$$

However, to account for both lines in the cutset failing simultaneously due to the occurrence of FT3 and/or FT4 of an adjacent line also in the cutset, we must create an added dependency mode failure rate, given in (17). The expected restoration time of a dependency mode failure is given in (18). See [12] for further reference on these adjustments. If the lines are not adjacent, the elements $\{x, y\}$ and $\{y, x\}$ in the probability matrices will be zero, and hence all adjustments and the dependency mode failure rate will be zero. The equivalent annual failure rate, expected annual unavailability and expected restoration time for the cutset is then calculated in (19)-(21).

$$\lambda_{x,y}^D = \lambda_{x,y}^a + \lambda_{y,x}^a \quad (17)$$

$$r_{x,y}^D = \begin{cases} \left(U_{x,y}^a + U_{y,x}^a\right)/\lambda_{x,y}^D & \text{if } \lambda_{x,y}^d > 0 \\ 0 & \text{Otherwise} \end{cases} \quad (18)$$

$$\lambda'_{x,y} = \frac{(\lambda'_x - \lambda^a_{x,y})(\lambda'_y - \lambda^a_{y,x})[r^n_{x,y} + r^n_{y,x}]}{8760} + \lambda^D_{x,y} \quad (19)$$

$$U'_{x,y} = \frac{(\lambda'_x - \lambda^a_{x,y})(\lambda'_y - \lambda^a_{y,x})[r^n_{x,y} \cdot r^n_{y,x}]}{8760} + \lambda^D_{x,y} \cdot r^D_{x,y} \quad (20)$$

$$r'_{x,y} = \frac{U'_{x,y}}{\lambda'_{x,y}} \quad (21)$$

B. Time series method

Time series of failure probability can be used to incorporate varying failure probabilities due to exposure to external threats, e.g. wind, lightning, icing etc., leading to failure bunching effects. For time series, unavailability and associated reliability indices for transmission lines are calculated using the time series of different fault types, dependent on adjacency. We therefore do not wish to calculate equivalent failure rates, repair rates or unavailability in the previously presented approximate manner, however, we wish to establish time-series of failure probabilities. We rely on the algorithmic method outlined in [8] to calculate resulting unavailability and further reliability indices.

The addition of a time dimension to failure rates makes it necessary to make alterations to the equations above. However, since the probability of a failure propagating is assumed not time dependent, we can continue using the same probability matrices already established in Section III. Rather than annual failure rates for transmission lines, we now consider time-series of hourly failure probabilities as presented in (22). When referring to the time-series of failure probability for a single line, we denote this column vector $\boldsymbol{\lambda}_{:,l}$. The fault types for a single line is given in (23)-(26).

$$\boldsymbol{\lambda}_{t,l} = \begin{bmatrix} \lambda_{1,1} & \cdots & \lambda_{1,l} \\ \vdots & \ddots & \vdots \\ \lambda_{t,1} & \cdots & \lambda_{t,l} \end{bmatrix} \quad (22)$$

$$\boldsymbol{FT1}_{:,i} = \boldsymbol{\lambda}_{:,l} \quad (23)$$

$$\boldsymbol{FT2}_{:,i} = [ft2_{t,i}], \text{ where } ft2_{t,i} = \frac{\sum_s \boldsymbol{\lambda}^s_l}{8760} \quad (24)$$

$$\boldsymbol{FT3}_{:,i} = \sum_j [\boldsymbol{\lambda}_{:,j} \cdot pt3_{i,j}] \quad (25)$$

$$\boldsymbol{FT4}_{:,i} = \sum_j [\boldsymbol{\lambda}_{:,j} \cdot pt4_{i,j}] \quad (26)$$

When calculating second order cutsets we need to adjust FT3 and FT4 to account for adjacency as we did for annual indices, for both lines x and y, as seen in (27)-(28). We also need to calculate a time series of dependency mode failure probability for the two lines in conjunction (29). Again, the adjustments are equal to zero if the lines are not adjacent. For the cutset itself, we calculate the unavailability of individual lines with updated fault type values separately using the method outlined in [8] before multiplying the results and adding the dependency mode unavailability.

$$\boldsymbol{FT3}^{\boldsymbol{a}}_{:,\boldsymbol{x}} = \boldsymbol{FT1}_{:,\boldsymbol{y}} \cdot pt3_{x,y} \quad (27)$$

$$\boldsymbol{FT4}^{\boldsymbol{a}}_{:,\boldsymbol{x}} = \boldsymbol{FT1}_{:,\boldsymbol{y}} \cdot pt4_{x,y} \quad (28)$$

$$\boldsymbol{\lambda}^{\boldsymbol{d}}_{\boldsymbol{x},\boldsymbol{y}} = \boldsymbol{FT1}_{:,\boldsymbol{y}} \cdot pt3_{x,y} + \boldsymbol{FT1}_{:,\boldsymbol{y}} \cdot pt4_{x,y} + \boldsymbol{FT1}_{:,\boldsymbol{x}} \cdot pt3_{y,x} + \boldsymbol{FT1}_{:,\boldsymbol{x}} \cdot pt4_{y,x} \quad (29)$$

IV. Case study

A test case is constructed to exemplify the impact on power systems reliability by taking the combined effect of failure bunching due to weather and protection system failures into account. The test case is based on the topology from the Roy Billinton Test System (RBTS) [24] with added protection systems, as shown in Fig. 2. A contingency enumeration approach [17] is employed to evaluate the reliability of the system. A consequence analysis of the contingencies was performed in [25] using a DC OPF algorithm, yielding interrupted power at load points for the different cutsets. This is used together with the unavailability of the cutsets to calculate their respective contributions to annual ENS of the system.

Unavailability of the different cutsets are calculated in four ways: 1) A base case using an approximate method of reliability evaluation not including protection system failures [18]. 2) An approximate method including protection systems failures, as outlined in Section III.A. 3) A time-series method including wind-dependent failure rates, as outlined in [8]. 4) A time-series method including wind-dependent failure rates [8] adjusted for protection system faults, as outlined in Section III.B. A simplification is done compared to the original approach in [8], and restoration times are assumed to be constant values, rather than distributions.

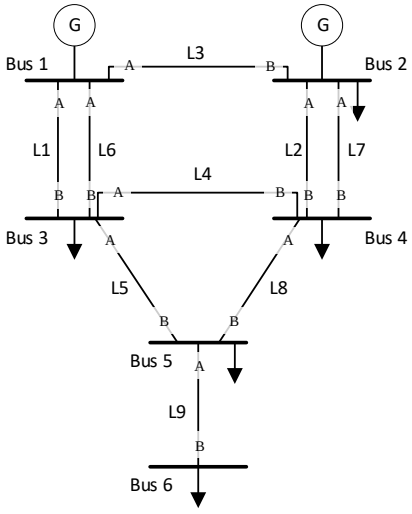

Fig. 2. RBTS [24] with added protection systems.

Topology, failure rates and dependent failure probabilities of lines are given in Table 1. Average annual failure rates for transmission lines are kept the same as Permanent Outage Rates (POR) in [24] for both methods, and all line failures have a 10 hour outage duration, to keep consistent with the original RBTS line data. Time series of hourly probability of failure due to wind is calculated according to the method outlined in [13], covering 25 years of hourly estimated failure probabilities due to wind for actual lines in the Norwegian transmission system. For the time-series of failure probabilities, 75 percent of the failure probability is assumed to be constant, while 25 percent is scaled wind dependent failure probability varying at an hourly interval. Repair of protection system units, relevant to FT2, are assumed to take 2 hours. FT3 and FT4 is associated with a 0.5 hour switching time.

TABLE 1: TRANSMISSION LINE INFORMATION

l	Bus connection A-side (u)	Bus connection B-side (v)	λ_l	λ_l^s	$P_l^{s,m}$	$P_l^{s,u}$
1	1	3	1.5	0.025	0.0205	0.007
2	2	4	5.0	0.025	0.0205	0.007
3	1	2	4.0	0.025	0.0205	0.007
4	3	4	1.0	0.025	0.0205	0.007
5	3	5	1.0	0.025	0.0205	0.007
6	1	3	1.5	0.025	0.0205	0.007
7	2	4	5.0	0.025	0.0205	0.007
8	4	5	1.0	0.025	0.0205	0.007
9	5	6	1.0	0.025	0.0205	0.007

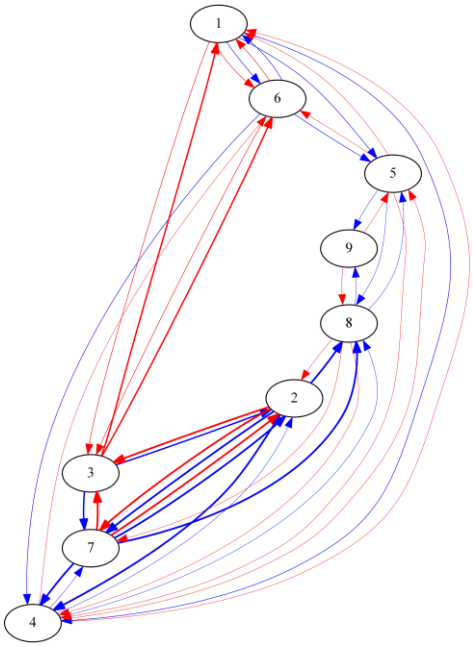

Fig. 3. Propagation graph for RBTS.

Adjacency matrices are created and weighted according to dependent probabilities and failure rates according to the procedure in Section III to incorporate protection system reliability into the analysis. The results can be illustrated as in Fig. 3, where vertices are transmission lines and the directed edges show the adjacency between the lines. The color of the edges indicates the source line protection system side (A-side is red, B-side is blue). The width of the edges corresponds to the contribution of failures to the target line, found at the arrowhead. To accumulate results, all edges leading into a vertex is summed up to see the contribution of FT3 and FT4 from the adjacent lines, as illustrated for line 6 in Fig. 4. Note the double connection between line 1 and 6 appearing, causing line 1 to contribute to FT3 and FT4 at line 6 through two separate paths.

The calculated fault types for each line are shown in Table 2, as well as the proportion of the incoming failures from neighboring lines in FT3 and FT4 as a share of the line's own fault type, FT1. Note the relatively large increase of annual failures on line 4, which is connected to four other lines, two of which, lines 2 and 7, have relatively high failure rates compared to the target line. This shows the potentially large impact on annual failure rates of a line from the number of incident lines and proximity to high-failure rate lines.

TABLE 2: FAULTS PER YEAR, FAULT TYPES

l	FT1	FT2	Incoming faults FT3	Incoming faults FT4	FT3 + FT4 % of FT1
1	1.5	0.05	0.18	0.12	20 %
2	5.0	0.05	0.33	0.22	11 %
3	4.0	0.05	0.27	0.18	11 %
4	1.0	0.05	0.31	0.20	51 %
5	1.0	0.05	0.12	0.08	20 %
6	1.5	0.05	0.18	0.12	20 %
7	5.0	0.05	0.33	0.22	11 %
8	1.0	0.05	0.27	0.18	44 %
9	1.0	0.05	0.04	0.03	7 %

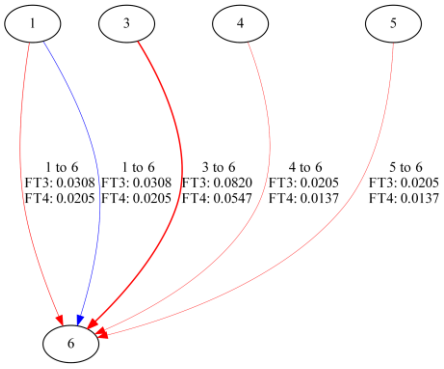

Fig. 4: Contributions to FT3 and FT4 from adjacent lines for target line 6. Annual values.

Table 3 shows the percentage change in annual ENS due to the different cutsets when different methods are employed, compared to the base case. Including protection system failures in the approximate method cause a large increase in annual ENS due to the cutset when the cutset contains two adjacent lines, with a 402 and 304 percent increase for cutsets {1,6} and {5,8}, respectively. The impact of including protection system failures on cutsets including single lines or two non-adjacent lines is limited due to short restoration times and low failure rates of protection systems compared to the line's own failure rate, and no dependency mode failure rate.

Employing the time series method including wind-dependent failure rates have no impact on the contribution to annual ENS from single line cutsets, as it merely moves the probability of when failures occur to different times of the year while the average annual unavailability for the line remains the same. However, overlapping periods of harsh weather for two lines cause the probability of the associated second order cutset to occur to be larger, leading to an increase in annual ENS of up to 119 percent in our test case compared to when failure bunching effects are not considered.

The effect of including both wind dependent failure rates and protection system failures leads to an increase of annual ENS up to 480 percent for second order cutsets containing adjacent lines, compared to the base case. Protection system failures are more likely to occur in periods of harsh weather, and the dependency mode failure rate shared between adjacent lines can have a large impact on expected unavailability of the cutset in certain time-periods. This is illustrated in Fig 5, where a 150-hour time window of hourly expected unavailability for the cutset {1,6} is presented with and without inclusion of protection system faults.

TABLE 3: PERCENTAGE CHANGE IN ANNUAL ENS [MWH/Y] DUE TO CUTSETS, FROM BASE CASE[a].

Cutset	A-PS[b]	T-W[c]	T-W+PS[d]
6,7	2 %	63 %	65 %
2,6	2 %	63 %	65 %
1,7	2 %	53 %	54 %
1,6	402 %	78 %	480 %
1,2	2 %	52 %	54 %
5,8	304 %	119 %	422 %
9	1 %	0 %	1 %

[a.] Approximate method, not including protection system failures.

[b.] Approximate method, including protection system failures.

[c.] Time-series method, including wind-dependent failure rates.

[d.] Time-series method, including protection system failures and wind dependent failure rates.

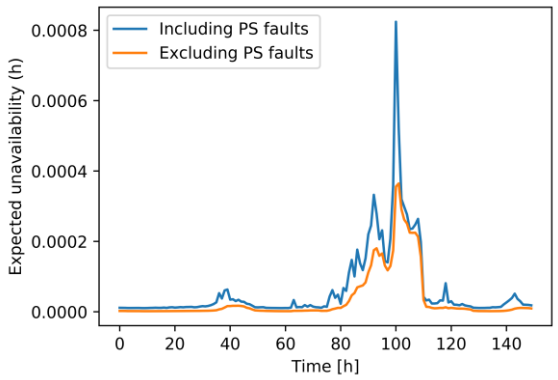

Fig 5: Cutset {1,6}. 150-hour window of hourly expected unavailability with and without including protection system (PS) faults.

V. CONCLUSION

In this paper we have shown a compact and generalized method of including protection system failures in power system reliability analysis, based on a graph-theoretical approach. The method was extended further to account for time-series of failure probability in the analysis, allowing for inclusion of time-varying failure probabilities throughout the year due to e.g. weather exposure.

A case study was presented to show the effect on reliability of supply when weather exposure and protection system maloperation were implemented into the analysis. The case study shows that taking protection system reliability and the adjacency of transmission lines into account can have a large impact on the contribution to annual ENS from certain cutsets due to the propagation of protection system failures. Since protection system maloperation follows an initial failure, propagating failures cluster around periods of high failure probability from other causes, and further increase risks associated with failure bunching effects. Thus, taking a time-series approach to capture time-varying failure rates including protection system failures can more accurately identify time-periods and sets of transmission lines which potentially have a high impact on the reliability of supply. Such an approach would be especially relevant when considering multiple operating states throughout the year. The method presented can be used to prioritize preventive and corrective measures aiming to reduce risks associated with unwanted events in the power system.

REFERENCES

[1] E. Bompard, T. Huang, Y. Wu, and M. Cremenescu, "Classification and trend analysis of threats origins to the security of power systems," *Int. J. Electr. Power Energy Syst.*, vol. 50, pp. 50–64, Sep. 2013.

[2] Y. Wang, C. Chen, J. Wang, and R. Baldick, "Research on Resilience of Power Systems Under Natural Disasters—A Review," *IEEE Trans. Power Syst.*, vol. 31, no. 2, pp. 1604–1613, Mar. 2016.

[3] M. Panteli and P. Mancarella, "Influence of extreme weather and climate change on the resilience of power systems: Impacts and possible mitigation strategies," *Electr. Power Syst. Res.*, vol. 127, pp. 259–270, Oct. 2015.

[4] P. Pourbeik, P. S. Kundur, and C. W. Taylor, "The anatomy of a power grid blackout," *IEEE Power Energy Mag.*, vol. 4, no. 5, pp. 22–29, Sep. 2006.

[5] P. Hines, J. Apt, and S. Talukdar, "Large blackouts in North America: Historical trends and policy implications," *Energy Policy*, vol. 37, no. 12, pp. 5249–5259, Dec. 2009.

[6] R. Billinton, G. Singh, and J. Acharya, "Failure Bunching Phenomena in Electric Power Transmission Systems," *Proc. Inst. Mech. Eng. Part O J. Risk Reliab.*, vol. 220, no. 1, pp. 1–7, Jan. 2006.

[7] M. Panteli and P. Mancarella, "Modeling and Evaluating the Resilience of Critical Electrical Power Infrastructure to Extreme Weather Events," *IEEE Syst. J.*, vol. 11, no. 3, pp. 1733–1742, 2017.

[8] E. S. Kiel and G. H. Kjølle, "Transmission line unavailability due to correlated threat exposure," in *Powertech [Accepted]*, Italy, 2019.

[9] H. Guo, C. Zheng, H. H.-C. Iu, and T. Fernando, "A critical review of cascading failure analysis and modeling of power system," *Renew. Sustain. Energy Rev.*, vol. 80, pp. 9–22, Dec. 2017.

[10] I. Dobson and D. E. Newman, "Cascading blackout overall structure and some implications for sampling and mitigation," *Int. J. Electr. Power Energy Syst.*, vol. 86, pp. 29–32, Mar. 2017.

[11] A. G. Phadke and J. S. Thorp, "Expose hidden failures to prevent cascading outages [in power systems]," *IEEE Comput. Appl. Power*, vol. 9, no. 3, pp. 20–23, Jul. 1996.

[12] V. V. Vadlamudi, O. Gjerde, and G. H. Kjølle, "Dependability and security-based failure considerations in protection system reliability studies," in *IEEE PES ISGT Europe 2013*, Denmark, 2013, pp. 1–5.

[13] Ø. R. Solheim, T. Trötscher, and G. H. Kjølle, "Wind dependent failure rates for overhead transmission lines using reanalysis data and a Bayesian updating scheme," in *PMAPS 2016*, 2016, pp. 1–7.

[14] R. Billinton, C. Wu, and G. Singh, "Extreme adverse weather modeling in transmission and distribution system reliability evaluation," presented at the PSCC, Sevilla, 2002.

[15] Ø. R. Solheim, L. Warland, and T. Trötscher, "A holistic simulation tool for long-term probabilistic power system reliability analysis," in *PMAPS 2018*, Boise, ID, 2018.

[16] G. H. Kjølle and O. Gjerde, "Integrated approach for security of electricity supply analysis," *Int. J. Syst. Assur. Eng. Manag.*, vol. 1, no. 2, pp. 163–169, Jun. 2010.

[17] O. Gjerde, G. H. Kjølle, S. H. Jakobsen, and V. V. Vadlamudi, "Enhanced method for reliability of supply assessment - an integrated approach," in *2016 PSCC*, Genoa, Italy, 2016, pp. 1–7.

[18] R. Billinton and R. N. Allan, *Reliability Evaluation of Power Systems*, Second Edition. New York, NY, USA: Plenum Press, 1996.

[19] Ke Sun, "Complex Networks Theory: A New Method of Research in Power Grid," in *2005 IEEE/PES Transmission Distribution Conference & Exposition: Asia and Pacific*, China, 2005, pp. 1–6.

[20] S. Arianos, E. Bompard, A. Carbone, and F. Xue, "Power grid vulnerability: A complex network approach," *Chaos Interdiscip. J. Nonlinear Sci.*, vol. 19, no. 1, p. 013119, Mar. 2009.

[21] G. A. Pagani and M. Aiello, "The Power Grid as a complex network: A survey," *Phys. Stat. Mech. Its Appl.*, vol. 392, no. 11, pp. 2688–2700, Jun. 2013.

[22] R. Diestel, *Graph Theory*, vol. 173. Berlin, Heidelberg: Springer Berlin Heidelberg, 2017.

[23] G. Chartrand and P. Zhang, *A first course in graph theory*, Dover ed. Mineola, NY: Dover Publications, 2012.

[24] R. Billinton *et al.*, "A reliability test system for educational purposes-basic data," *IEEE Trans. Power Syst.*, vol. 4, no. 3, pp. 1238–1244, Aug. 1989.

[25] A. G. Jensen, "Weather Models for Capturing Wind Related Failures in Probabilistic Reliability Analysis of Power Systems," Master thesis, NTNU, Trondheim, Norway, 2019.